World Journal of Advanced Research and Reviews
eISSN: 2581-9615 CODEN (USA): WJARAI
Cross Ref DOI: 10.30574/wjarr
Journal homepage: https://wjarr.com/

(RESEARCH ARTICLE)

Check for updates

STRUCTURE-BASED OPTIMIZATION OF DRILLING AND BLASTING PARAMETERS USING AIR DECKS, BOREHOLE VIDEO LOGGING AND UAV-BASED FRAGMENTATION ASSESSMENT AT THE VASILKOVSKOYE GOLD DEPOSIT, KAZAKHSTAN

Daulet Kuatovich Takhanov, Merei Zhumagalievna Balpanova, Aibar Kuatovich Blyal and Aigerim Temirgalievna Karabatyrova *

Scientific and Technical Center of Industrial Safety LLP, Karaganda, Republic of Kazakhstan.
* Corresponding Author

ORCID Details
Daulet Kuatovich Takhanov: https://orcid.org/0000-0002-2360-9156
Merei Zhumagalievna Balpanova: https://orcid.org/0000-0002-1513-5317
Aibar Kuatovich Blyal: https://orcid.org/0009-0002-1006-3569
Aigerim Temirgalievna Karabatyrova: https://orcid.org/0009-0005-4335-7610

World Journal of Advanced Research and Reviews, 2026, 32(02), 1467–1477

Publication history: Received on 12 October 2026; revised on 16 November 2026; accepted on 18 November 2026

Article DOI: https://doi.org/10.30574/wjarr.2026.32.2.2979

Copyright © 2026 Author(s) retain the copyright of this article. This article is published under the terms of the Creative Commons Attribution License 4.0

ABSTRACT

This study aimed to optimize drilling and blasting parameters at the Vasilkovskoye open-pit gold mine (Kazakhstan), where very strong rock (UCS ≈ 118 MPa), intersecting fault systems and groundwater complicate blast design. The methodology combined analysis of the structural model, borehole video logging of 250 blast holes in six pilot blocks, stereographic interpretation of joint orientations, a parametric model of decked charges with gas-inflated air-deck bags (Blastbag), production blasts in eight blocks (four with air decks and four with continuous charges; ≈460,000 m^3) and digital image analysis of UAV photographs of the muck piles. Four structural domains with dominant NE-striking (VASIL) and NW-striking (DONG) joint sets were delineated, and initiation against the dip of the dominant set was recommended. Across the eight blocks, the median fragment size depended mainly on the powder factor (P50 ≈ 691 – 526q, r ≈ −0.78), so group differences cannot be attributed to the air deck. A paired comparison within one block, at identical drill pattern and initiation, showed that a 0.4 m air deck (≈7% of the explosive column) reduced the explosive mass by 10.3 kg per hole while keeping P20 and P50 within 1.6% and 0.1% of the continuous charge, reducing P80 by 9.4% and increasing P99 by 22.0%. Blastbags performed reliably in water-filled holes. Direct explosive savings were about 1.35 million KZT per 100,000 m^3, with a projected 2.61–3.92 million KZT for air decks of 14–21% of the column. The technology reached TRL 7 and was adopted by the operator.

Keywords: Air-deck blasting; Blastbag; Borehole video logging; Unmanned aerial vehicle; Rock fragmentation; Vasilkovskoye deposit

1 INTRODUCTION

Drilling and blasting is the first link of the mine-to-mill chain, and the size distribution of the blasted rock directly affects the productivity and cost of excavation, haulage, crushing and grinding. Because explosives are one of the main cost items of blast preparation, reducing the powder factor without degrading fragmentation is a practical objective at most open-pit mines [1–3].

Blast outcomes are strongly controlled by the structure of the rock mass. In jointed rock, a large part of the final fragmentation is inherited from the in-situ block size, whereas in massive rock a greater share of explosive energy is needed to create new fracture surfaces [4–6]. The orientation of the dominant joint sets relative to the free face and the direction of initiation also governs the opening of natural discontinuities, back-break and the stability of the remaining bench [1]. Consequently, uniform blast parameters applied to a structurally heterogeneous rock mass tend to produce uneven fragmentation, oversize and excessive explosive consumption.

Air-deck blasting, developed by Melnikov and Marchenko, is one of the established methods for managing the distribution of explosive energy in a blast hole [7]. An air gap in the charge column reduces the peak borehole pressure and prolongs the action of the detonation products on the rock through repeated reflections of pressure waves; in the original experiments, explosive consumption was reduced by 10–30% without deterioration of fragmentation [7, 8]. Subsequent field studies in jointed rock [9], quarry trials [10], Russian production studies [11] and numerical simulations [12, 13] confirmed the potential of the method, and a top air deck placed beneath the stemming was shown to improve fragmentation in the collar zone [14]. Gas-inflated bags have made air decking practical in production, and industrial case studies report lower explosive costs and reduced ground vibration [15, 16].

However, the recommended air-deck parameters (typically 0.15–0.35 of the charge length and a specific position in the column) were obtained for particular geological conditions and cannot be transferred to very strong, structurally heterogeneous and water-bearing rock masses without field verification [8–10]. Furthermore, in production trials the effect of the charge design is usually confounded with simultaneous changes in drill pattern, powder factor and geology, which makes it difficult to isolate. Digital image analysis of fragmentation [17–19] and unmanned aerial vehicles (UAVs) now allow block-scale evaluation of blast results, while the Kuz-Ram [20] and Swebrec [21] models provide a basis for prediction and calibration.

The objective of this study was to develop and justify measures for optimizing drilling and blasting parameters at the Vasilkovskoye deposit based on structural characterization of the rock mass by borehole logging, the use of air decks formed with Blastbag devices and UAV-based fragmentation assessment. The specific tasks were (i) to delineate structural domains and relate them to the initiation direction; (ii) to formulate a parametric description of decked charges; (iii) to conduct production trials and isolate the effect of the air deck by an intra-block paired comparison; and (iv) to evaluate the economic effect. The working hypothesis was that rational placement of an air deck, accounting for the structural domain, reduces explosive consumption while maintaining technologically acceptable fragmentation.

2 MATERIAL AND METHODS

The study followed the workflow shown in Figure 1: geological and structural data were combined with borehole video logging to delineate structural domains, decked charges were parameterized and tested in production blasts, and the results were evaluated by UAV-based fragmentation analysis and an economic assessment that feeds back into the charge design.

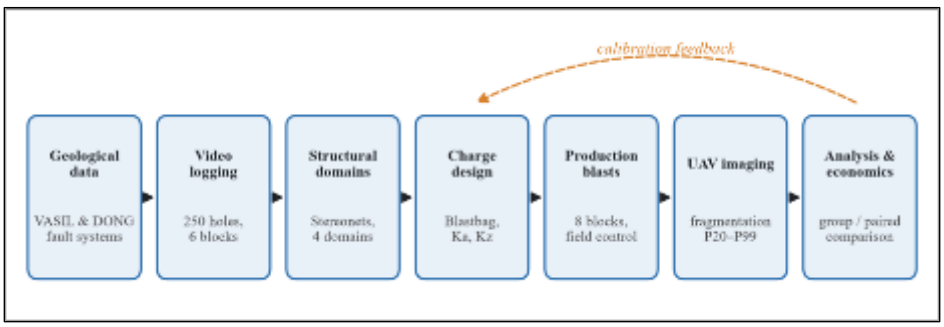


Figure 1: Research workflow

2.1 Study site

The Vasilkovskoye gold deposit is located in northern Kazakhstan and is mined by open pit by Altyntau Kokshetau JSC. It is confined to a belt of hybrid rocks in the endocontact zone of the Altybay granite massif with Lower Proterozoic metamorphic rocks. The gold–sulphide–quartz stockwork is hosted by granodiorites and gabbro-diorites and is overlain by a Mesozoic weathering crust 10–65 m thick. The ore and host rocks are very strong (R_c = 1200 kgf/cm^2, ≈118 MPa) and contain 66.2–89.4% silica. Fissure and fissure-vein groundwater occurs to a depth of 550 m (375 m on average), so a considerable proportion of blast holes are water-filled.

The structural framework is formed by two regional fault systems. The older VASIL system strikes NE–NNE, dips steeply to the SE and has predominantly sinistral kinematics; the younger DONG system strikes NW–NNW, dips steeply to the WSW–SW and is dextral, cross-cutting and partly transposing VASIL structures. An earlier system of moderately dipping normal faults (Moderate structure) is also present. The intersections of VASIL and DONG are the most disturbed parts of the rock mass.

2.2 Borehole video logging and structural domains

Optical televiewer logging was initially planned, but water turbidity, small-block structure in the upper benches and silted hole walls prevented acquisition of usable images. Therefore, video logging was carried out with a downhole camera equipped with a cable winch and a depth counter. A total of 250 holes (diameter 165 mm, depth 10–11 m) were logged in six pilot blocks (26-195-13, 26-205-8, 26-185-5, 26-185-4, 26-175-7 and 26-195-20) in a staggered pattern with a spacing of about 10 m (every third or fourth hole). Open and partly open fractures, intensely fractured and crushed intervals, cavities, wall instability and water inflows were recorded over the full bench height.

The logging results were combined with the existing structural model and field mapping. Dip direction and dip of the structural surfaces were processed statistically using stereographic projections and rose diagrams [4]. The pit was divided into four structural domains based on the spatial distribution of measurements and geological features, and a geomechanical model of the pilot blocks was synthesized.

2.3 Parametric model of the decked charge

To compare holes of different depth and design, the charge geometry was described by a length balance:

$$L_h = L_{ch} + L_a + L_{st} + L_{int} \qquad (1)$$

where L_h is the actual hole depth, L_{ch} the total length of explosive decks, L_a the total air-deck length, L_{st} the top stemming length and L_{int} the total length of inter-deck stemming (all in m). The explosive mass per hole Q_h (kg) and the powder factor q (kg/m^3) are

$$Q_h = \Sigma\, \lambda_i \cdot L_{ch,i}\,, \quad q = \Sigma Q_h \,/\, V_b \qquad (2)$$

where λ_i is the linear charge concentration of deck i (kg/m) and V_b is the blasted volume (m^3). The air deck is characterized by two dimensionless parameters, its relative length K_a and the relative depth of its centre K_z:

$$K_a = L_a \,/\, L_h\,, \quad K_z = z_a \,/\, L_h \qquad (3)$$

where z_a is the depth of the air-deck centre from the collar. This parameterization replaces the binary attribute "with/without Blastbag" by the actual charge geometry.

Two decked-charge designs were implemented with a bulk emulsion-based explosive (Fortis Extra 70, density 1.20 g/cm^3) (Figure 2). In Variant 1, a 0.4 m air deck was placed beneath the top stemming above a continuous bottom column (10.3 = 5.6 + 0.4 + 4.3 + 0 m; K_a = 0.0388, K_z = 0.4369; λ = 25.66 kg/m). In Variant 2, the charge was divided into two decks separated by inter-deck stemming (4.3–5.3 m) and a 0.4 m air deck (5.3–5.7 m) (9.3 = 5.1 + 0.4 + 2.8 + 1.0 m; K_a = 0.0430, K_z = 0.5914; λ = 27.53 and 27.56 kg/m for the upper and lower decks). The air decks were formed by gas-inflated Blastbag devices lowered to the design depth before loading.

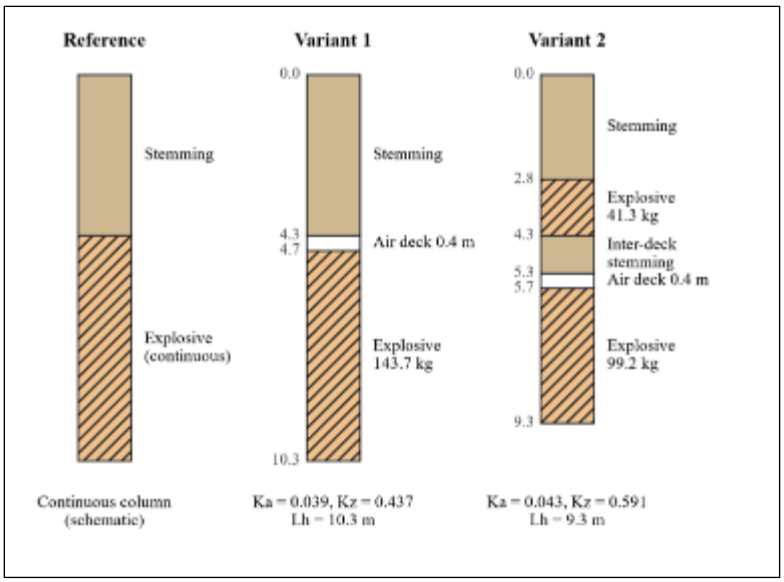


Figure 2: Charge designs: reference continuous column (schematic) and the two decked-charge variants with Blastbag air decks (depths from the collar, m)

2.4 Production blast trials

Production blasts were carried out in eight blocks between 6 August and 19 October 2026, with a total volume of about 460,000 m^3 and 1,688 holes of 165 mm diameter (Table 1). The air-deck group (blocks 26-195-13, 26-205-8, 26-185-5 and 26-185-4) was blasted in August and the control group with continuous charges (26-175-7, 26-195-20, 26-175-10 and 26-195-21) in October. In addition, block 26-205-8 was divided into a zone with Blastbag and a zone without Blastbag that had the same hole diameter, drill pattern (5.2 × 6.0 m), bench level, geology, initiation scheme and image-analysis procedure. The block was initiated with a V-pattern designed in ShotPlus, with a delay of 5–15 ms per metre of burden in the main part of the block and 15–25 ms/m at its ends.

Table 1: Technological parameters of the trial blocks (hole diameter 165 mm in all blocks)

Block	Blast date	Charge type	Pattern B × S, m	Area per hole, m^2	q, kg/m^3
26-195-13	06.08.2026	Blastbag	5.4 × 6.2	33.5	0.472
26-205-8	11.08.2026	Blastbag + zone without	5.2 × 6.0	31.2	0.438
26-185-5	18.08.2026	Blastbag	5.1 × 5.9	30.1	0.579
26-185-4	20.08.2026	Blastbag	5.2 × 6.0	31.2	0.500
Air-deck group	Aug 2026	Variants 1 and 2	5.1 × 5.9 – 5.4 × 6.2	31.5	0.497
26-175-7	02.10.2026	Continuous	4.9 × 5.6	27.4	0.697
26-195-20	13.10.2026	Continuous	4.9 × 5.6	27.4	0.666
26-175-10	16.10.2026	Continuous	4.9 × 5.6	27.4	0.695
26-195-21	19.10.2026	Continuous	4.9 × 5.6	27.4	0.736
Control group	Oct 2026	Continuous column	4.9 × 5.6	27.4	0.699

Note: q for block 26-205-8 refers to the whole block, including the zone without Blastbag.

Field control was carried out together with the charging contractor. In the controlled holes, hole depth was measured before charging, the Blastbag depth was recorded at installation, and the top of the charge and stemming length were measured after loading; the explosive mass was taken from the mobile manufacturing unit records. Hole conditions (water, short or blocked holes, wall fracturing), stemming quality and all operations were documented by photographs and video (Figure 3).



Figure 3: Installation of a Blastbag at the design depth in a production blast hole

2.5 UAV imaging and fragmentation analysis

Before the flights, a reconnaissance of each site was performed to identify obstacles (equipment, power lines, dumps), select take-off and landing sites and check weather conditions; the wind speed did not exceed the limit of 12 m/s. A DJI Air 3S quadcopter with a fixed-focal-length camera was used to photograph each block before and after blasting. The images were sorted by block and date, checked for completeness and quality, and suitable images of the muck piles were analysed with WipFrag 4 [19]. The fragmentation was characterized by P20, P50, P80 and P99 (fragment sizes below which 20, 50, 80 and 99% of the material passes) and by the proportion of material finer than 200 mm (F200). For blocks 26-195-13, 26-185-5 and 26-185-4, the values are averages of two analysed zones. Because the ground sampling distance, RTK/GCP use and RMSE were not documented, no orthomosaics or surface models were produced, and the results are treated as image-based fragmentation estimates.

2.6 Data analysis and economic evaluation

Two comparison schemes were used. The between-group comparison characterizes the overall blasting regime of the air-deck group (pattern, powder factor and charge design together). The intra-block paired comparison on block 26-205-8 isolates the effect of the charge design; the relative change of each indicator was calculated as

$$\Delta P_i = (P_{i,BB} - P_{i,0}) / P_{i,0} \times 100\% \qquad (4)$$

where $P_{i,BB}$ and $P_{i,0}$ are the values in the zones with and without Blastbag. A linear regression between P50 and q was fitted for all eight blocks and its residuals were compared between groups.

The explosive mass replaced by the air deck, the corresponding reduction in powder factor and the net direct effect per hole were calculated as

$$\Delta Q = \lambda \cdot L_a\,, \quad \Delta q_{BB} = \Delta Q / (a \cdot H)\,, \quad \Delta E = \Delta Q \cdot C_e - C_{BB} \qquad (5)$$

where a is the area per hole (m^2), H the bench height (m), C_e the cost of 1 kg of explosive including delivery and charging (407.66 KZT/kg) and C_{BB} the cost of one installed Blastbag. With a = 31.2 m^2 and H = 10 m, one hole breaks 312 m^3, i.e. about 321 holes per 100,000 m^3. Prospective savings of 20–30 kg per hole were evaluated for zones of different rock strength.

3 RESULTS

3.1 Structural domains and initiation direction

The stereographic analysis showed that steeply dipping joint sets related to the regional faults dominate in all four domains, but their orientation changes systematically from one domain to another (Table 2). The Northern domain has a compact pole cluster indicating a well-defined principal set with low scatter. In the Eastern domain, the regional structural orientation associated with the major faults is most clearly expressed, with steep sets dipping S–SE and

somewhat greater scatter. The Southern and Western domains show the greatest scatter, with additional secondary sets that indicate higher structural heterogeneity.

Table 2: Orientation of the main fault and joint systems by structural domain

Domain	Structural system	Strike azimuth, °	Dip direction, °	Dip, °
Northern wall	Set N-1	320–340	050–070	70–85
	Set N-2	300–320	030–050	60–80
Eastern wall	VASIL-1	040–060	130–150	65–85
	DONG-1	320–340	050–070	70–85
Southern wall	DONG-1	300–320	210–230	70–90

Video logging of 42 holes in block 26-175-7 (transition-zone rocks) showed relatively homogeneous rock with intact, cylindrical hole walls; only minor cavities and locally rough intervals (e.g. hole No. 87) were observed, and no extensive zones of intense fracturing or open faults were detected. However, short and blocked holes, holes with fractured walls and loss of explosive into open fractures were encountered during charging in other blocks, so the favourable conditions of block 26-175-7 cannot be extrapolated to all blocks.

Based on the orientation of the dominant sets, an initiation principle was formulated (Figure 4): the blast front should propagate against the dip of the dominant joint set, so that the dynamic loading presses the joints together rather than opening them. For the Eastern wall, where structures dip predominantly to the SE, the front should propagate to the NW, with two free faces, one of which is on the initiation side.

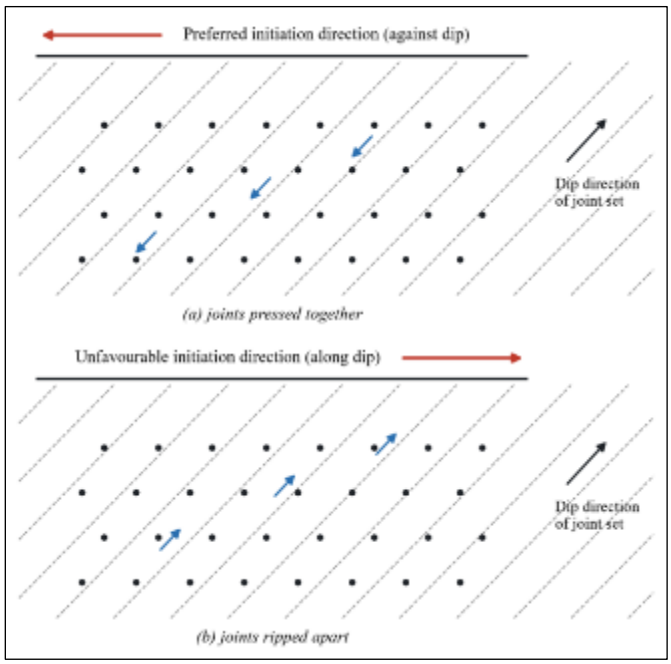


Figure 4: Effect of initiation direction relative to the dip of the dominant joint set: (a) preferred, (b) unfavourable

3.2 Field implementation of the decked charges

In the controlled holes, the Blastbags were fixed at the design depth, retained their position during explosive loading and formed air decks of the design length, including in water-filled holes. The applicability of the decked charges with Blastbag was therefore confirmed in both dry and water-filled holes using standard drilling and charging equipment. The deviations recorded were short and blocked holes, holes with fractured walls, loss of explosive into open fractures, and stemming material with a heterogeneous grain size containing coarse inclusions. These deviations could cause the actual explosive mass, deck lengths and stemming to differ from the design values and were considered in the interpretation.

3.3 Between-group comparison

The air-deck group was blasted with a mean powder factor of 0.497 kg/m^3, 28.8% lower than the control group (0.699 kg/m^3), and with a 14.8% larger area per hole. Under these conditions, the air-deck group produced coarser fragmentation (Table 3): P20, P50, P80 and P99 were higher by 23.7%, 31.1%, 43.6% and 17.3%, respectively, and F200 was lower by 7.14 percentage points.

Table 3: Fragmentation indicators of the trial blocks

Group	Block	P20, mm	P50, mm	P80, mm	P99, mm	F200, %
Air deck	26-195-13	249.24	544.93	933.23	1248.46	14.33
Air deck	26-185-5	186.59	353.60	699.22	1038.04	22.50
Air deck	26-185-4	165.25	381.42	942.73	1211.83	26.19
Air deck	26-205-8 *	213.14	430.67	718.19	1189.04	17.92
Mean	Air-deck group	203.56	427.66	823.34	1171.84	20.24
Control	26-175-7	168.29	337.91	571.07	958.35	25.53
Control	26-195-20	150.08	309.70	618.57	1051.59	30.30
Control	26-175-10	166.14	329.20	599.29	1165.47	27.22
Control	26-195-21	173.46	328.04	504.22	820.97	26.46
Mean	Control group	164.49	326.21	573.29	999.10	27.38

* Zone with Blastbag; the zone without Blastbag is excluded from the group means and is used in Section 3.4.

A linear regression over all eight blocks gave P50 ≈ 691 − 526q (P50 in mm, q in kg/m^3; r ≈ −0.78), showing that the median fragment size decreases with increasing powder factor (Figure 5). The mean residuals were −2.2 mm for the air-deck group and +2.1 mm for the control group, and the estimated contribution of the lower powder factor to the between-group difference in P50 was +105.8 mm. However, the powder factor ranges of the groups do not overlap (0.438–0.579 and 0.666–0.736 kg/m^3), so the slope is determined mainly by the between-group difference, and the residual difference of −4.3 mm cannot be interpreted as an effect of the charge design. The between-group comparison therefore characterizes the combined blasting regime and does not allow the effect of Blastbag to be isolated.

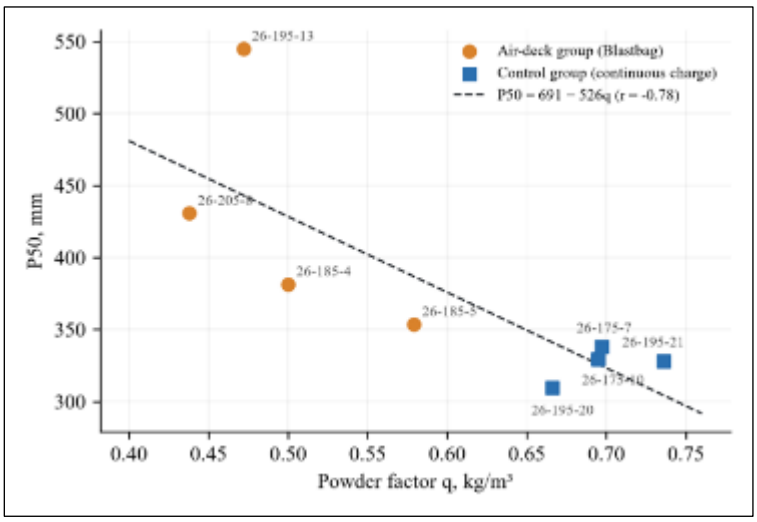


Figure 5: Median fragment size P50 versus powder factor *q* for the eight trial blocks

3.4 Intra-block paired comparison

On block 26-205-8, the Blastbag replaced 0.4 m of the explosive column, which at λ = 25.66 kg/m reduced the charge by about 10.3 kg per hole. P20 and P50 in the two zones were practically identical (+1.6% and +0.1%), and F200 changed by only −0.58 percentage points (Table 4, Figure 6). In the zone with Blastbag, P80 decreased from 792.43 to 718.19 mm (−9.4%), whereas P99 increased from 974.63 to 1189.04 mm (+22.0%), indicating the presence of individual coarse

fragments in the analysed sample. The comparison is based on a single pair of zones without replication and thus indicates a trend that requires confirmation.

Table 4: Fragmentation in the zones with and without Blastbag on block 26-205-8

Indicator	Without Blastbag	With Blastbag	Change
P20, mm	209.85	213.14	+3.29 mm (+1.6%)
P50, mm	430.32	430.67	+0.35 mm (+0.1%)
P80, mm	792.43	718.19	−74.24 mm (−9.4%)
P99, mm	974.63	1189.04	+214.41 mm (+22.0%)
F200, %	18.50	17.92	−0.58 p.p.

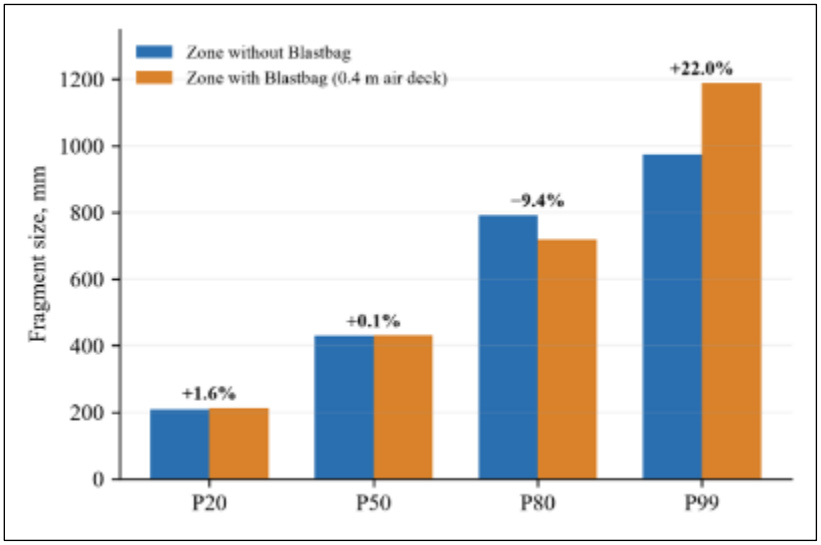


Figure 6: Fragmentation indicators in the zones with and without Blastbag on block 26-205-8

3.5 Explosive savings and economic effect

Table 5: Estimated explosive savings with Blastbag per 100,000 m³ (one Blastbag per hole, a = 31.2 m², H = 10 m)

Scenario	ΔQ, kg/hole	L_a, m	Share of column, %	Δq_{BB}, kg/m³	Saving, t	Value, KZT
Actual (block 26-205-8)	10.3	0.40	7.1	0.033	3.30	1,345,686
Strong, slightly fractured rock	20	0.78	13.9	0.064	6.41	2,613,101
Average conditions	25	0.97	17.4	0.080	8.01	3,266,580
Weaker, highly fractured rock	30	1.17	20.9	0.096	9.62	3,919,651

Note: values exclude the cost of Blastbag; the 20–30 kg/hole scenarios are projections that require field confirmation.

The between-group reduction in powder factor (0.201 kg/m³, or 20.1 t of explosive per 100,000 m³) reflects the entire blasting regime of the air-deck group and cannot be regarded as a saving due to Blastbag. The saving attributable to the air deck itself is $\Delta Q = 25.66 \times 0.4 \approx 10.3$ kg per hole, which for block 26-205-8 corresponds to $\Delta q_{BB} \approx 0.033$ kg/m³, or about 3.3 t per 100,000 m³ (≈16% of the between-group reduction). At C_e = 407.66 KZT/kg, the value of the saved explosive is about 4,199 KZT per hole; hence, Blastbag is economically justified if its installed cost is below this value ($C_{BB} < \lambda \cdot L_a \cdot C_e$).

Increasing the explosive saving to 20–30 kg per hole would require air decks of 0.78–1.17 m, i.e. 14–21% of the 5.6 m explosive column, which is close to the lower part of the range recommended in the literature. The lower bound corresponds to strong, slightly fractured rock and the upper bound to zones of lower strength and higher fracturing. Under these conditions, the break-even cost of an installed Blastbag rises 2–3-fold, to 8,153–12,230 KZT, and the value of saved explosive reaches 2.61–3.92 million KZT per 100,000 m^3 (Table 5).

4 DISCUSSION

The intra-block comparison supports the working hypothesis: an air deck reduced the explosive mass by about 7% without a measurable deterioration of P20–P80. This is consistent with the mechanism described in the literature, whereby an air gap lowers the peak pressure of the detonation products, extends their duration of action and distributes energy more evenly along the bench height [7, 8, 13]. In very strong rock, the effect on the median size was negligible, while the decrease in P80 suggests better breakage of the coarse fraction in the charged part of the bench. The increase in P99 indicates that the largest fragments originate from the upper part of the bench and the stemming zone, which is also where heterogeneous stemming material with coarse inclusions was observed. A top air deck placed directly beneath the stemming has been shown to improve collar-zone fragmentation [14], which justifies comparing top and mid-column air-deck positions in further trials.

The air deck used in the trials (≈7% of the explosive column) was 2–4 times shorter than the commonly recommended 15–35% of the charge length [8, 9]; in quarry trials, 20–30% was recommended and up to 40% under favourable conditions [10]. This explains both the weak influence on P50 and the limited saving compared with the 10–30% reduction reported in classical studies [7] and the 20–24% reduction in explosive cost reported for gas-bag air decks in granitic rock at a gold mine [15]. At the same time, numerical modelling shows that increasing the air-deck length beyond a rational value raises the pressure on the stemming and the flyrock velocity [12], so a longer air deck must be accompanied by control of stemming length and quality. Russian production studies also indicate that the mean fragment size obtained with air-decked charges decreases as the rock becomes more difficult to blast [11], which supports continued trials in the strong rocks of the deposit.

The study also demonstrates a methodological point. The between-group comparison mixed the effects of a 29% lower powder factor, a 15% larger pattern, different blasting periods and different geology, and the regression of P50 on q could not separate these factors because the powder factor ranges did not overlap. Only the paired comparison within one block, at constant pattern and initiation, isolated the effect of the charge design. This supports the "one cycle – one variable" principle for optimization: when possible, the drill pattern should be kept constant while the air-deck position, air-deck length, stemming length, charge mass and delay timing are adjusted sequentially.

The results have several limitations: the intra-block comparison is based on a single pair of zones without replication; the air-deck and control groups were blasted in different periods; the as-drilled collar coordinates were not surveyed, and the powder factor was calculated from the design block volume; oversize yield, floor condition, crest loss, back-break and peak particle velocity (PPV) were not measured; the UAV imagery lacked documented ground sampling distance and georeferencing; video logging covered six of the eight blocks; and compliance of the actual initiation sequence with the recommended direction remains to be verified.

For industrial implementation, a staged approach is recommended. First, the result of block 26-205-8 should be confirmed by repeated paired trials, starting with blocks under comparable conditions and zones of lower strength and higher fracturing, where the saving potential is highest. The air-deck length should then be increased stepwise from 0.4 m to about 15% and 25% of the explosive column at a constant pattern, and the top position beneath the stemming should be tested, with control of stemming length, P99, flyrock distance and PPV. A domain-based matrix "structural domain → Blastbag design → fragmentation → geotechnical indicators → PPV → recommended charge design" should be maintained, and every controlled hole should be recorded "as built" (collar position, depth, Blastbag position, air-deck length, explosive mass, stemming length and water) to enable "design → execution → result" analysis. Literature data indicate that air decks can reduce ground vibration by 35–50%, throw by 20–35% and back-break by 16–25% [8], and gas bags in trim rows have helped to achieve final-wall criteria [22] and reduce flyrock [23]; therefore, separate trials in the rows nearest to final walls with instrumented PPV monitoring are justified. Calibration of the Kuz-Ram [20] and Swebrec [21] models against UAV-based measurements, and numerical modelling of single holes and hole groups, will support the transition to TRL 8.

5 CONCLUSION

An integrated approach combining structural characterization, decked charges with Blastbag and UAV-based fragmentation assessment was developed and tested at the Vasilkovskoye gold deposit. The main findings are as follows:

- Borehole video logging of 250 holes in six pilot blocks, combined with the structural model and stereographic analysis, delineated four structural domains with dominant VASIL and DONG joint sets; initiation against the dip of the dominant set (to the NW on the Eastern wall) is recommended.
- A parametric model of the decked charge based on the length balance and the dimensionless parameters K_a and K_z allows the actual charge geometry, rather than a binary "with/without air deck" attribute, to be analysed and holes of different depth to be compared.
- For the eight production blocks, the empirical relation $P50 \approx 691 - 526q$ ($r \approx -0.78$) shows that the powder factor dominates the between-group difference in median size; the between-group comparison therefore characterizes the overall blasting regime and not the effect of the air deck.
- In the intra-block paired comparison, a 0.4 m air deck ($K_a \approx 0.04$) reduced the explosive mass by 10.3 kg per hole, kept P20 and P50 at the level of the continuous charge, reduced P80 by 9.4% and increased P99 by 22.0%. Blastbags performed reliably in water-filled holes.
- The direct explosive saving is about 4,199 KZT per hole, or 1.35 million KZT per 100,000 m^3, and is projected to reach 2.61–3.92 million KZT per 100,000 m^3 with air decks of 14–21% of the column; Blastbag is justified when its installed cost is below the value of the explosive it replaces.

The technology has been demonstrated at TRL 7, accepted for implementation by Altyntau Kokshetau JSC (implementation certificate No. 7 of 28 October 2026) and protected by a utility model patent of the Republic of Kazakhstan [24]. Further work should confirm the results with replicated paired trials, longer and top-positioned air decks, and instrumented monitoring of PPV, wall condition and oversize.

STATEMENTS ON COMPLIANCE WITH ETHICAL STANDARDS

Acknowledgments

The study was carried out by Scientific and Technical Center of Industrial Safety LLP under Contract No. 3120/2026-0707 of 20 April 2026 with Altyntau Kokshetau JSC. The authors thank B. R. Rakhmetov, A. B. Rymkulova and B. S. Bakir (Scientific and Technical Center of Industrial Safety LLP) for their participation in the field work and data processing, and the specialists of Altyntau Kokshetau JSC and the charging contractor for their support during the field work.

The research was also carried out by order of Zhairem Mining and Processing Plant JSC (Zhairem GOK) under Contract No. 3110/2026-1787 of 13 August 2026, within the topic "Study of the geological structure of the rock mass using optical logging and UAV-based fragmentation assessment for optimization of drilling and blasting parameters", in accordance with the terms of reference for the research work (basis: Research Plan of Zhairem GOK JSC for 2026).

Funding Source

This research was funded by Altyntau Kokshetau JSC (Contract No. 3120/2026-0707 of 20 April 2026) and Zhairem Mining and Processing Plant JSC (Contract No. 3110/2026-1787 of 13 August 2026).

Disclosure of conflict of interest

The research was funded by Altyntau Kokshetau JSC, the operator of the Vasilkovskoye mine, and by Zhairem Mining and Processing Plant JSC (Zhairem GOK). D. K. Takhanov, M. Zh. Balpanova and A. K. Blyal are co-inventors of the utility model patent cited in this article, and D. K. Takhanov is the patent holder. The authors declare no other conflicts of interest.

REFERENCES

[1] Konya CJ, Walter EJ. Surface blast design. Englewood Cliffs (NJ): Prentice Hall; 1990.

[2] Hustrulid W. Blasting principles for open pit mining. Vols 1–2. Rotterdam: A.A. Balkema; 1999.

[3] Persson PA, Holmberg R, Lee J. Rock blasting and explosives engineering. Boca Raton (FL): CRC Press; 1994.

[4] Priest SD. Discontinuity analysis for rock engineering. London: Chapman & Hall; 1993.

[5] Hoek E, Brown ET. Practical estimates of rock mass strength. Int J Rock Mech Min Sci. 1997;34(8):1165–1186.

[6] Barton N, Lien R, Lunde J. Engineering classification of rock masses for the design of tunnel support. Rock Mech. 1974;6(4):189–236.

[7] Melnikov NV, Marchenko LN. Effective methods of application of explosion energy in mining and construction. In: Clark GB, editor. Dynamic rock mechanics. Proceedings of the 12th Symposium on Rock Mechanics. New York: AIME; 1971. p. 350–378.

[8] Sazid M, Singh TN. Mechanism of air deck technique in rock blasting: a brief review. In: Proceedings of the Fourth Indian Rock Conference (INDOROCK 2013); 2013. Available from: https://www.researchgate.net/publication/257924487

[9] Jhanwar JC, Jethwa JL, Reddy AH. Influence of air-deck blasting on fragmentation in jointed rocks in an open-pit manganese mine. Eng Geol. 2000;57(1–2):13–29.

[10] Rommayawes S, Leelasukseree C, Jaroonpattanapong P. Influence of air-deck length on fragmentation in quarry blasting. Eur Sci J. 2014. Available from: https://eujournal.org/index.php/esj/article/view/2426

[11] Overchenko MN, Tolstunov SA, Mozer SP, Belin VA. Optimal parameters of process flows in air-decoupling blasting. Mining Informational and Analytical Bulletin. 2022;(4):87–99. doi:10.25018/0236_1493_2022_4_0_87

[12] Arefmand E, Bakhshandeh Amnieh H, Majdi A. Numerical analysis of the impact of air column length on the rock mass damage zone in air deck blasting operation. Int J Min Geo-Eng. 2025;59(3):247–253. doi:10.22059/IJMGE.2025.381451.595191

[13] Hawinkel J, et al. Improving blast outcomes: why airdecks work — a numerical modeling study. In: Proceedings of the Annual Conference on Explosives and Blasting Technique. Cleveland (OH): International Society of Explosives Engineers; 2025.

[14] Kabwe E. Improving collar zone fragmentation by top air-deck blasting technique. Geotech Geol Eng. 2017;35(1):157–167. doi:10.1007/s10706-016-0094-7

[15] Avane S, Wilson-Sey J, Niminye A, Anani A, Aderuyi S. Blast optimization using air decking with gasbags – an open pit gold mine case study. In: Proceedings of the Annual Conference on Explosives and Blasting Technique. Cleveland (OH): International Society of Explosives Engineers; 2025.

[16] MTi Group. Maximizing your profits with air decking [Internet]. Case study. [cited 2026 Nov 19]. Available from: https://www.shop.mtigroup.us/blogs/case-studies/maximizing-your-profits-with-air-decking

[17] Kemeny J, Devgan A, Hagaman R, Wu X. Analysis of rock fragmentation using digital image processing. J Geotech Eng. 1993;119(7):1144–1160.

[18] Sanchidrián JA, Segarra P, López LM. A practical procedure for the measurement of fragmentation by blasting by image analysis. Rock Mech Rock Eng. 2006;39(4):359–382.

[19] Maerz NH, Palangio TC, Franklin JA. WipFrag image based granulometry system. In: Franklin JA, Katsabanis T, editors. Measurement of blast fragmentation. Rotterdam: A.A. Balkema; 1996. p. 91–99.

[20] Cunningham CVB. The Kuz-Ram model for prediction of fragmentation from blasting. In: Holmberg R, Rustan A, editors. Proceedings of the First International Symposium on Rock Fragmentation by Blasting; 1983; Luleå, Sweden. Luleå: Luleå University of Technology; 1983. p. 439–453.

[21] Ouchterlony F. The Swebrec function: linking fragmentation by blasting and crushing. Min Technol. 2005;114(1):29–44.

[22] MTi Group. Optimising trim blasting [Internet]. Case study. [cited 2026 Nov 19]. Available from: https://www.mtigroup.com.au/case-studies/optimising-trim-blasting

[23] MTi Group. Flyrock reduction in surface blasting [Internet]. Case study. [cited 2026 Nov 19]. Available from: https://www.shop.mtigroup.com.au/blogs/case-studies/flyrock-reduction-in-surface-blasting

[24] Takhanov DK, Balpanova MZh, Blyal AK, Balabaev OT. Method of creating air cavities in blast holes. Utility model patent of the Republic of Kazakhstan, IPC F42D 1/08. Application No. 2026/1298.2, filed 2026 Jun 9; decision to grant 2026 Oct 29.